

Regular Article

# Nonsteroidal ecdysone receptor agonists use a water channel for binding to the ecdysone receptor complex EcR/USP

Christopher Browning,<sup>1,2,3,4,#</sup> Alastair G. McEwen,<sup>1,2,3,4</sup> Kotaro Mori,<sup>5</sup> Taiyo Yokoi,<sup>5,§</sup> Dino Moras,<sup>1,2,3,4</sup> Yoshiaki Nakagawa<sup>5</sup> and Isabelle M. L. Billas<sup>1,2,3,4,\*</sup>

<sup>1</sup> Centre for Integrative Biology (CBI), Department of Integrated Structural Biology, IGBC (Institute of Genetics and of Molecular and Cellular Biology), Illkirch, France

<sup>2</sup> Centre National de la Recherche Scientifique (CNRS), UMR 7104, Illkirch, France

<sup>3</sup> Institut National de la Santé et de la Recherche Médicale (INSERM), U1258, Illkirch, France

<sup>4</sup> Université de Strasbourg, Strasbourg, France

<sup>5</sup> Graduate School of Agriculture, Kyoto University, Kyoto 606–8502, Japan

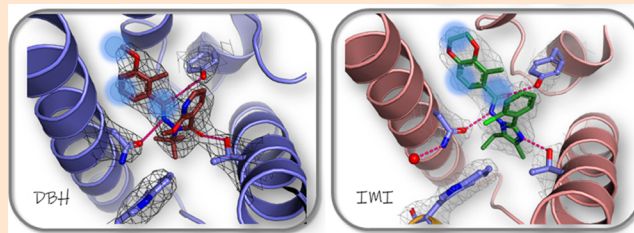
<sup>#</sup> Present address: Vertex Pharmaceuticals, 86–88 Jubilee Avenue Milton Park, Abingdon Oxfordshire OX14 4RW, UK

<sup>§</sup> Present address: Sagami Chemical Research Institute, Ayase 252–1193, Japan

(Received December 25, 2020; Accepted January 16, 2021)

## Supplementary material

The ecdysone receptor (EcR) possesses the remarkable capacity to adapt structurally to different types of ligands. EcR binds ecdysteroids, including 20-hydroxyecdysone (20E), as well as nonsteroidal synthetic agonists such as insecticidal dibenzoylhydrazines (DBHs). Here, we report the crystal structures of the ligand-binding domains of *Heliothis virescens* EcR/USP bound to the DBH agonist BYI09181 and to the imidazole-type compound BYI08346. The region delineated by helices H7 and H10 opens up to tightly fit a phenyl ring of the ligands to an extent that depends on the bulkiness of ring substituent. In the structure of 20E-bound EcR, this part of the ligand-binding pocket (LBP) contains a channel filled by water molecules that form an intricate hydrogen bond network between 20E and LBP. The water channel present in the nuclear receptor bound to its natural hormone acts as a critical molecular adaptation spring used to accommodate synthetic agonists inside its binding cavity.



**Keywords:** ecdysone receptor, ligand-binding domain, structural adaptation, water channel, dibenzoylhydrazine, imidazole.

## Introduction


The steroid hormone 20-hydroxyecdysone (20E) (Fig. 1) plays a crucial role in the regulation of molting, metamorphosis, reproduction, and an array of developmental processes in insects and in arthropods.<sup>1–3)</sup> 20E acts on the ecdysone receptor (EcR) which forms a heterodimer with USP, the arthropod homologue

of the vertebrate RXR.<sup>4–9)</sup> Since EcR is absent in vertebrates, ligand molecules of EcRs have the potential for the development of insect specific insecticides. Dibenzoylhydrazine (DBH)-type compounds are representative nonsteroidal ligands and exhibit remarkable insect toxicity.<sup>10,11)</sup> Although they share no structural and chemical similarity with ecdysteroids, they are capable of binding to EcR with high affinity and bring about premature molting, leading to the larval death of lepidopteran and certain coleopteran insects. Interestingly, however, they are ineffective against some other insect groups. DBHs are constituted by two benzoyl moieties, bridged through a *tert*-butylated hydrazide linker.<sup>10,12–14)</sup> Quantitative structure–activity relationship (QSAR) studies targeting these three parts revealed that A- and B-ring substitutions confer different insect species specificities.<sup>15–17)</sup> In particular, substitutions on the A-ring were shown to be essential to distinguish broad-spectrum lepidopteran and

\* To whom correspondence should be addressed.

E-mail: billas@igbmc.fr

Published online February 4, 2021

 © Pesticide Science Society of Japan 2021. This is an open access article distributed under the Creative Commons Attribution-NonCommercial-NoDerivatives 4.0 International (CC BY-NC-ND 4.0) License (<https://creativecommons.org/licenses/by-nc-nd/4.0/>)

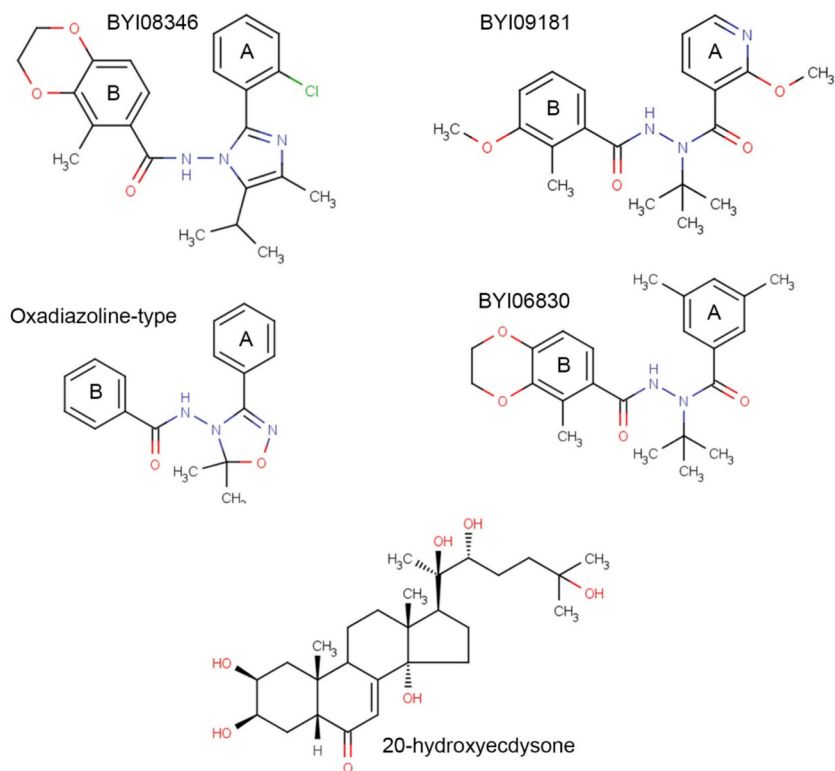


**Fig. 1.** Chemical structures of synthetic ecdysone agonists and the natural hormone 20-hydroxyecdysone (20E). Depicted are the dibenzoylhydrazine (DBH) compounds BYI06830 (Bayer CropScience) and BYI09181 (Bayer CropScience) and the imidazole-type compound BYI08346 (Bayer CropScience) and an oxadiazoline-type of compounds (OXA)

coleopteran specificity from strict lepidopteran specificity.<sup>18)</sup>

Several crystal structures of the ligand-binding domains (LBDs) of EcR/USP have been published, a few for the moth *Heliothis virescens* (HvEcR/HvUSP),<sup>19,20)</sup> for the beetle *Tribolium castaneum* (TcEcR/TcUSP),<sup>21)</sup> for the whitefly *Bemisia tabaci* (BtEcR/BtUSP)<sup>22)</sup> and more recently for the phthirapteran *Bovicola ovis* (BoEcR/BoUSP).<sup>23)</sup> In addition, the cryo electron microscopy structure of the full receptor HvEcR/HvUSP bound to a natural DNA response element was solved at medium resolution.<sup>24)</sup> The structure gave key information on the topological organization of the domains with respect to the palindromic response elements. In addition, the secondary structure elements observed in the crystal structures of the HvEcR/HvUSP LBDs could be readily seen in the electron density map, suggesting that the observations made for the LBD homodimer are preserved in the full receptor bound to DNA. From the ligand point of view, most of the structures were solved for the heterodimer in complex with ecdysteroids, namely ponasterone A (PonA) or 20E. Two crystal structures have so far been reported in complex with ecdysone agonists, namely that of HvEcR/HvUSP bound to the DBH insecticide BYI06830<sup>19,25)</sup> and that of BoEcR/BoUSP bound to the weak agonist methylene lactam which was not observed in the crystal structure of BoEcR, being either disordered or absent from the pocket.<sup>23)</sup> On the other hand, the structure of HvEcR bound to BYI06830 provided insight into nuclear receptor adaptation to ligand binding, since it was shown to be mark-

edly different from the structure of HvEcR bound to PonA or 20E. In fact, a drastic structural rearrangement of the ecdysone receptor was observed upon binding of the smaller DBH ligand at the level of the  $\beta$ -sheet and of helices H2, H7 and H10.

In this paper, we present the crystal structures of HvEcR/HvUSP bound to two novel high affinity nonsteroidal ecdysone agonists, BYI09181 and BYI08346, where BYI09181 is a typical DBH insecticide compound like BYI06830, while BYI08346 represents a modified DBH compound, where the *t*-butyl amide part of the DBH compound is replaced by a substituted imidazole ring. Despite chemical differences between these ligands, we show here that EcR binds BYI09181 and BYI08346 in a way similar to what is observed for BYI06830. In addition, the two structures of HvEcR/HvUSP bound to nonsteroidal ecdysone agonists BYI09181 and BYI08346 provide more detailed information on the binding modes of these synthetic agonists to EcR and allow to unravel the molecular mechanisms of the structural adaptation of the receptor to ligand binding. In particular we show that the synthetic agonists specifically bind in a region of the ligand-binding pocket (LBP) that is occupied by structural water molecules that form a water channel when the natural ligand is bound inside the pocket.

## Materials and methods

### 1. Protein expression, purification and crystallization

The LBDs of HvEcR (residues 284–532) and HvUSP (resi-

dues 205-466) were co-expressed in the same bacterial host *Escherichia coli*, BL21 (DE3) on separate vectors, with the expression of HvEcR/HvUSP in complex with the synthetic ligands making use of a quadruple mutant of HvEcR (W303Y, A316S, L456S, C483S) as previously described.<sup>19)</sup> Quadruple mutant HvEcR was fused to a His6-tag and expressed in the pET-28b vector with ampicillin resistance. HvUSP was expressed in the pACYC-11b vector with chloramphenicol resistance. The cultures were carried out at 37°C and induced with IPTG and continued at 18°C for 18 hr. Cells were harvested by centrifugation, pellets re-suspended in 4°C sterile water, and centrifuged for 20 min at 4000 rpm. For each 5 mL of cell pellet, 25 mL of lysis buffer (20 mM Tris pH 8.0, 500 mM NaCl, 10% glycerol, 2 mM CHAPS) was added and the pellet was re-suspended in presence of 40  $\mu$ M ligand and sonicated. Soluble protein was extracted by ultra-centrifugation and the crude extract was loaded onto a 5 mL, Ni-HighTrap metal affinity chromatography column (GE Healthcare). Elution of the protein was carried out with lysis buffer containing 250 mM imidazole. The His6-tag was removed with thrombin digestion, and final polishing of the protein (20 mM Tris pH 8.0, 50 mM NaCl, 150 mM KCl, 2% glycerol, 4 mM CHAPS) was achieved with gel-filtration using a HiLoad 16/60 Superdex 75 column (GE Healthcare). The purified protein was concentrated to a final concentration of 7–8 mg/mL. Purity of protein was assessed with SDS and native polyacrylamide gel electrophoresis, dynamic light scattering, native and denaturant electrospray ionization mass spectrometry. Crystallization was carried out using the hanging drop vapour diffusion method using a 2  $\mu$ L protein + 2  $\mu$ L reservoir drop size. The reservoir contained 500  $\mu$ L crystallization buffer. Crystals were obtained in around 5 days from a reservoir condition containing 20% PEG 3350, and 0.2 M MgCl<sub>2</sub>, for HvEcR/HvUSP bound to BYI09181 at 24°C, forming hexagonal plates with dimensions around 200  $\times$  200  $\times$  30  $\mu$ m<sup>3</sup>. HvEcR/HvUSP bound to BYI08346 was crystallized at 24°C in a condition consisting of 10% PEG 1000, 10% PEG 8000, 0.3 M MgCl<sub>2</sub>, 0.1 M Hepes pH 7.5. Crystals formed within 3 days as hexagonal plates with dimensions around 300  $\times$  200  $\times$  80  $\mu$ m<sup>3</sup>.

## 2. Data processing, molecular replacement and structure refinement

Crystals for both BYI09181 and BYI08346 bound HvEcR/HvUSP were flash frozen in liquid ethane at liquid nitrogen temperature. Data were collected from single crystals for BYI09181 bound to HvEcR/HvUSP at the Swiss Light Source (SLS PX beamline) and for BYI08346 bound to HvEcR/HvUSP on beamline ID14-EH3 at the European Synchrotron Radiation Facility (ESRF, Grenoble, France). The observed reflections were processed to 3.05 Å and 2.85 Å for BYI09181 and BYI08346 respectively, using HKL2000.<sup>26)</sup> Crystals of HvEcR/HvUSP in complex with BYI09181 belong to the space group *P*<sub>3</sub><sub>2</sub><sub>1</sub> with cell dimensions *a*=147.035 *b*=147.035 *c*=162.306. Crystals of HvEcR/HvUSP in complex with BYI08346 belong to the space group *P*<sub>3</sub><sub>2</sub><sub>1</sub> with cell dimensions *a*=147.87

*b*=147.87 *c*=59.77. Details of the data are summarized in Table 1. Structures were determined with molecular replacement using MOLREP (for the BYI09181-bound EcR/USP)<sup>27)</sup> and AMoRE<sup>28)</sup> (for the BYI08346-bound EcR/USP), using the previously solved BYI06830 bound HvEcR/HvUSP structure (protein databank entry 1R20).<sup>19)</sup> Molecular replacement for BYI09181 produced a solution containing 3 heterodimers per asymmetric unit with the space group *P*<sub>3</sub><sub>2</sub><sub>1</sub>. The solution for the crystals of the BYI08346 bound HvEcR/HvUSP contains one molecule per asymmetric unit. Iterative cycles of crystallographic refinement and model building was carried out with CNS<sup>29)</sup> and O.<sup>30)</sup> Final rounds of refinement were carried out with the PHENIX suite,<sup>31)</sup> followed by iterative cycles of manual interventions in COOT.<sup>32)</sup> For the BYI09181 bound complex, the final model (corresponding to the 'h12' conformer), *R*<sub>work</sub> and *R*<sub>free</sub> are 0.19 and 0.24 respectively. For the BYI08346 bound complex, the final model (corresponding to the 'up' conformer) *R*<sub>work</sub> and *R*<sub>free</sub> are 0.17 and 0.22, respectively. Table 1 summarizes data collection and refinement statistics. Parameter and topology coordinates for ligands were generated with Grade (Global Phasing, <http://www.globalphasing.com>). Quality of the final models was monitored with MOLPROBITY,<sup>33)</sup> revealing no outliers in the Ramachandran plot. Protein cavity volume computation was carried out with VOIDOO.<sup>34)</sup> The EcR-LBD structures were superimposed using Lsq-man<sup>30)</sup> or using the PyMOL align command. Molecular graphics figures were generated using PyMOL Molecular Graphics System (DeLano Scientific, San Carlos, CA; [www.pymol.org](http://www.pymol.org)).

## 3. Molecular Dynamics simulations and MM/PBSA calculations

Molecular dynamics (MD) simulations and molecular mechanics/Poisson–Boltzmann surface area (MM/PBSA) calculations were executed according to the previously reported method with some modifications.<sup>35)</sup> The atomic coordinates for the EcR subunit and the ligand were extracted from each of the X-ray crystal structures. The missing residues and side chains were filled using MODELLER version 9.24. Ten models were generated for each ligand–receptor complex, and one with the lowest 'molpdf' score was selected as the initial structure for the MD simulations.

The AMBER18 software package was used for system preparation, MD simulations and MM/PBSA calculations. The *antechamber* module was used to calculate AM1-BCC charges for the ligands. The simulation systems were built using the *tleap* module. The ff14SB and GAFF2 force fields were used to describe the protein and the ligand, respectively. Na<sup>+</sup> and Cl<sup>−</sup> ions were added to neutralize the charge of the systems. The systems were immersed in the rectangular box of TIP3P water molecules that extends at least 10 Å from the solute surface.

MD simulations were performed using the *pmemd.cuda* module. Periodic boundary conditions were applied to all systems. The particle mesh Ewald method was employed to calculate the electrostatic interactions with a cutoff of 12.0 Å. The time step was set to 1 fs. The SHAKE algorithm was used to restrain co-

**Table 1.** Data collection and refinement statistics.

	BYI08346	BYI09181
Beamline	ESRF ID14-EH3	SLS PX
Detector	MARCCD	MARCCD
Wavelength (Å)	0.931	0.7749
Resolution range (Å)	46.48–2.85 (2.952–2.85)	48.13–3.05 (3.159–3.05)
Space group	$P 3_2 1$	$P 3_2 2 1$
Unit cell (Å)	147.875 147.875 59.776 90 90 120	147.035 147.035 162.306 90 90 120
Number of dimers in ASU	1	3
Unique reflections	17798 (1738)	37522 (3604)
Multiplicity	7.5	7.2
Completeness (%)	99.92 (99.94)	95.86 (93.97)
Mean I/sigma(I)	39.8 (7.0)	27.48 (5.49)
Wilson B-factor (Å <sup>2</sup> )	57.11	60.56
R-merge (%)	5.4 (33.8)	8.5 (46.9)
Reflections used in refinement	17798 (1739)	37522 (3602)
Reflections used for R-free	938 (100)	1880 (166)
R-work	0.1827 (0.2321)	0.1960 (0.2372)
R-free	0.2305 (0.2847)	0.2473 (0.3275)
Number of non-H atoms	4049	11762
macromolecules	3839	11420
ligands	122	250
solvent	88	92
Protein residues	479	1441
RMS(bonds)	0.002	0.002
RMS(angles)	0.46	0.40
Ramachandran favoured (%)	97.45	97.46
Ramachandran allowed (%)	2.34	2.47
Ramachandran outliers (%)	0.21	0.07
Rotamer outliers (%)	2.84	2.10
Clashscore	3.38	4.18
Average B-factor (Å <sup>2</sup> )	63.71	66.69
macromolecules (Å <sup>2</sup> )	63.84	66.81
ligands (Å <sup>2</sup> )	67.82	68.91
solvent (Å <sup>2</sup> )	52.23	46.19

Statistics for the highest-resolution shell are shown in parentheses.

valent bonds involving hydrogens. First, the systems were relaxed using steepest descent and conjugate gradient algorithms to achieve a gradient of  $<0.05 \text{ kcal mol}^{-1} \text{ Å}^{-2}$ . Next, the systems were gradually heated from 0 to 300 K in an NVT ensemble for 50 ps with a restraint of  $0.5 \text{ kcal mol}^{-1} \text{ Å}^{-2}$ . The systems were then equilibrated in an NPT ensemble for 900 ps. Production runs were performed in an NPT ensemble for 1.5 ns, during which the snapshots were stored every 10 ps. For each ligand–receptor complex, the MD simulation was performed in triplicate with different initial atomic velocities; thus 450 snapshots ( $150 \times 3$ ) per complex were collected for MM/PBSA calculations.

MM/PBSA calculations were performed using the *MMPBSA.py.MPI* module. The internal and external dielectric constants were set to 1.0 and 80.0, respectively. The ionic strength was set

to 0.2 mM. Entropy corrections were not made in this study.

## Results

### 1. Crystal structures of HvEcR/HvUSP bound to BYI09181 and BYI08346

The ligand binding domains of *Heliothis virescens* EcR (284–532, quadruple mutant, see Materials and Methods) and USP (205–466) were co-expressed in *E. coli*, purified to homogeneity and crystallized using hanging drop vapour diffusion method. The non-steroidal ecdysone agonists BYI09181 and BYI08346 were added at all steps of protein expression and purification. These compounds, depicted in Fig. 1, are strong ecdysone agonists (as shown in Suppl. Table 1) that bind specifically to lepidopteran EcR.<sup>36)</sup> BYI09181 is a representative insecticidal DBH



compound. The A-ring of BYI09181 is a pyridine ring that contains a 2-methoxy substitution, while the B-ring is a 2-methyl-3-methoxybenzene that is same as that of methoxyfenozide. On the other hand, BYI08346 represents a modified DBH molecule where the *tert*-butylated amide is replaced by an imidazole ring. In this respect, this molecule resembles oxadiazoline (OXA) compounds, in which an oxadiazole ring is present instead of the imidazole ring of BYI08346.<sup>18,37</sup>

Complexes of HvEcR/HvUSP with BYI09181 and with BYI08346 crystallized in two different space groups and data were collected to medium/high resolution at synchrotron beamlines. Structures were solved by using molecular replacement using the structure of HvEcR/HvUSP in complex with BYI06830 (PDB code 1R20), followed by iterative cycles of manual building and refinement (see Materials and Methods, Table 1). The overall structural shapes, depicted in Figs. 2A–B, of the HvEcR/HvUSP heterodimer in complex with BYI09181 and with BYI08346 are highly similar to the previously solved EcR/USP structures.<sup>19–22</sup> They form a typical heterodimer with a similar dimerization interface as the ones observed for vertebrate heterodimeric and homodimeric nuclear receptor LBDs.<sup>25</sup> The heterodimers are shaped like a butterfly when viewed from

the front. The interface of the two monomers is created between helices H7, H9, H10 and the loop between H8 and H9 (L8–9) and the two subunits are related by a pseudo C2 symmetry axis. For both structures, HvEcR and HvUSP have the canonical 3-layer sandwich anti-parallel helical nuclear receptor fold, with EcR resembling the structure of HvEcR LBD in complex with BYI06830. HvEcR is in the active agonist conformation, with helix H12 tightly folded up against the main body of the LBD. HvUSP adopts an antagonist conformation, as found in all the structures of this protein, isolated<sup>38</sup> or in heterodimer with HvEcR, in its LBD form<sup>19,20,39</sup> or as full protein on a DNA fragment from a typical EcR target gene.<sup>24</sup>

The BYI09181- and BYI08346-bound HvEcR structures resemble and superimpose well the structure of BYI06830-bound HvEcR with a root-mean-squared deviation (rmsd) of 0.62 Å for 207 C $\alpha$  atoms and 0.75 Å for 219 C $\alpha$  atoms, respectively. These three structures contrast with the structures of HvEcR in complex with 20E<sup>20</sup> and PonA.<sup>19</sup> While the latter feature a three-stranded  $\beta$ -sheet and a helix H2, the binding of synthetic agonists to EcR results in the unwinding of H2 into a loop and the disruption of the three-stranded  $\beta$ -sheet by the formation of interactions between residues of the erstwhile second and third

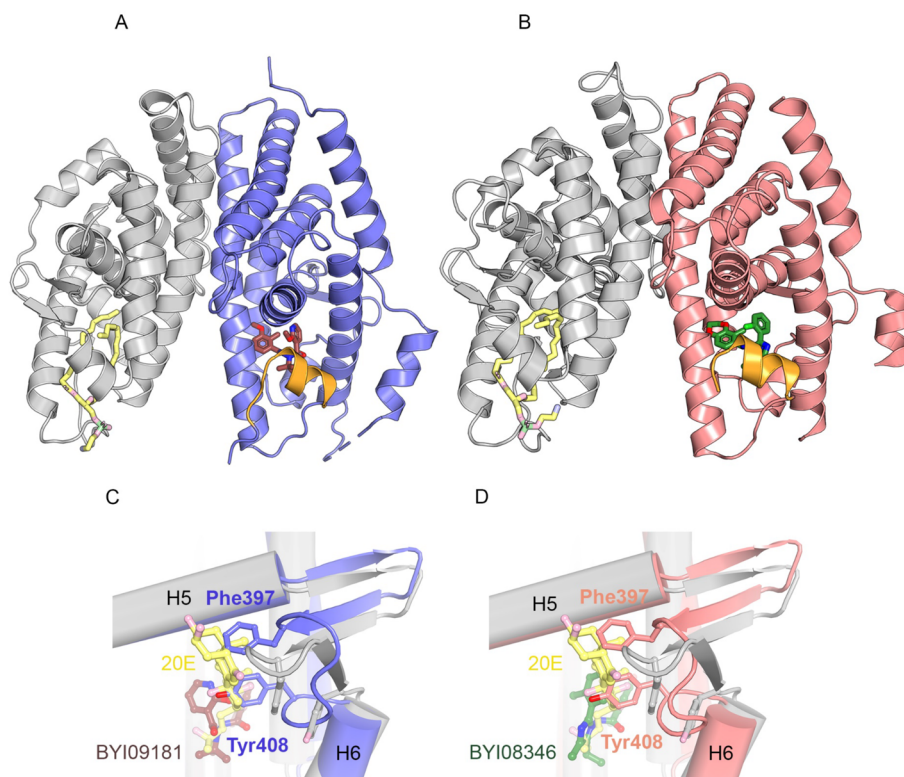


**Fig. 2.** The EcR LBD structurally adapts to the binding of synthetic agonists. (A–B) Overall view of the EcR/USP LBD structures in complex with (A) BYI09181 (slate) and (B) BYI08346 (salmon). The ligands are shown by stick models. Atom coloring is red for oxygen, blue for nitrogen, dark red for carbon in BYI09181 and green for carbon in BYI08346. The USP LBD is represented by grey ribbons with the phospholipid ligand represented as yellow sticks. (C–D) Ribbon diagram showing the superimposition of the structures of HvEcR-LBD in complex with (C) BYI09181 (slate) and 20E (grey) or (D) BYI08346 (salmon) and 20E (grey). The view shows to the region differing the most between the 20E- and synthetic agonist-bound EcR-LBDs that includes helices H2, H6, H7 and the  $\beta$ -sheet. The ligands are shown by stick models. Atom coloring is red for oxygen, blue for nitrogen, dark red for carbon in BYI09181, green for carbon in BYI08346 and yellow for carbon in 20E.

$\beta$ -strands. This rearrangement is the consequence of the inward motion of two aromatic residues Phe397 and Tyr403, located on each side of the  $\beta$ -sheet, that fill in the void created by the absence of the steroid core of ecdysteroids in this region (Figs. 2C and D).

## 2. *BYI09181 and BYI08346 fill a part of the pocket occupied by water molecules in the ecdysteroid-bound structures*

The structures of EcR in complex with BYI09181 and BYI08346 feature a Y-shaped LBP situated in the bottom half of the receptor embedded within the  $\alpha$ -helical sandwich and projecting towards helices H7 and H10 (Fig. 3A). The volume of the LBP of BYI08346 (494 Å<sup>3</sup>) which is slightly larger than that of BYI09181 (452 Å<sup>3</sup>) are comparable to the BYI06830 pocket (519 Å<sup>3</sup>). The difference between the volumes of the LBP of BYI08346 and BYI09181 are consistent with the larger size of BYI08346 (338 Å<sup>3</sup>) compared to BYI09181 (310 Å<sup>3</sup>). The overall position of BYI09181 and BYI08346 inside their respective LBP overlaps well with the position adopted by BYI06830 when bound to HvEcR (Fig. 3B), while overlapping partially with ecdysteroids at the level of their hydroxylated side chain, as shown in Fig. 3C. The A- and B-ring moieties of BYI09181, BYI08346 and BYI06830 are found globally in similar locations. However, the positioning of the moieties on the A- and B-ring of BYI08346 and BYI09181 cannot be determined in a clear-cut manner only from the corresponding electron density map. Several conformations would fit inside the electron density map and chemical considerations are necessary to discriminate between the different possibilities. This will be discussed in detail below. On the

other hand the positioning of the *tert*-butyl groups of BYI09181 and BYI06830 and that of the isopropyl group of BYI08346 is unambiguous. In fact, these functional groups superimpose well, except for a slight shift of the BYI06830 *tert*-butyl moiety (Fig. 3B). The imidazole ring of BYI08346 and its substitution at the 4-position are accommodated inside the LBP by a 1.2–1.4 Å outward shift of the N-terminal part of helices H3 and H6 and the loop H6-H7 (Fig. 3A), thus creating a slightly wider LBP at this place than in the case of the more classical DBH compounds, such as tebufenozide and halofenozide.

Finally, an important observation comes from the comparison of the occupancy of the LBP by the synthetic ligands and the ecdysteroids, as exemplified by 20E (Fig. 3D). The ecdysteroid binding inside the EcR cavity is always accompanied by the presence of structural water molecules in the region between helices H7 and H10, forming a water channel, linking, through H-bonds, the side chain hydroxyl groups of the ecdysteroid ligand and the pocket-lining residues. This hydrogen-bonding network helps maintaining helices H7 and H10 close together. In stark contrast with the case of the ecdysteroid-bound EcR, structural water molecules are totally absent from the cavity of synthetic ligand-bound EcR at this location for the simple reason that the pocket is occupied by the B-ring and its substituent, suggesting that this part of the synthetic ligands plays a structuring role buttressed mainly by van der Waals interactions. Notice that the distance between H7 and H10 is considerably larger in the case of synthetic ligands compared to that observed for ecdysteroid-bound EcR (by about 2 Å), consistent with the molding of the receptor to the bound synthetic ligand.

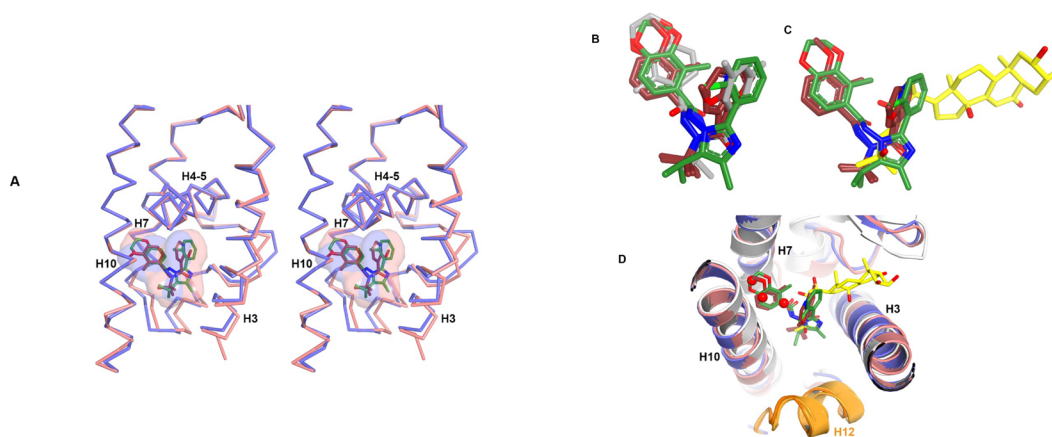


**Fig. 3.** Ligand-binding pockets and the water channel. (A) Stereoview of the ligand-binding pockets of EcR-LBD in complex with BYI09181 (pink ribbons) and BYI08346 (green ribbons). The BYI09181-bound EcR cavity is shown in light pink and the BYI08346-bound EcR cavity in light green. The ligands are shown by stick models. Atom coloring is red for oxygen, blue for nitrogen, pink for carbon in BYI09181 and green for carbon in BYI08346. (B) Superimposition of the synthetic agonists BYI09181, BYI08346 and BYI06830 as found in the LBP of EcR. BYI09181, BYI08346 and BYI06830 are shown in stick representation, with carbon atoms coloured in pink, green and grey, respectively, oxygen atoms in red, nitrogen atoms in blue. (C) Superimposition of the synthetic agonists BYI09181, BYI08346 and of the ecdysteroid 20E as found in the LBP of HvEcR. BYI09181, BYI08346 and 20E are shown in stick representation, with carbon atoms coloured in pink, green and gold, respectively, oxygen atoms in red, nitrogen atoms in blue. (D) Superimposition of the structures of EcR bound to BYI09181, BYI08346 and 20E, together with the three structural water molecules observed in the LBP of ecdysteroid-bound EcR structures. The view is restricted to the region of helices H7 and H10. The structure of HvEcR-LBD in complex with BYI09181, BYI08346 and 20E is depicted by blue, pink and grey ribbons, respectively.

3. *The binding of DBH- and imidazole-type compounds involves a similar pattern of H-bond interactions with residues of the HvEcR LBP*

Since all the synthetic ligands are located in a similar region of the ligand-binding pocket, their interaction with protein residues are rather similar, involving mainly H-bonds with three polar residues (Thr343, Tyr408 and Asn504) and a similar pattern of hydrophobic interactions (Fig. 4). For the classical DBH ligand BYI09181, strong hydrogen bonds are formed between the ligand and LBP residues, one between the carbonyl group close to the A-ring and the hydroxyl group of Thr343, another one between the amide nitrogen close to the B-ring and the side chain carbonyl group of Asn504 and finally a third one between the carbonyl group close to the B-ring and the hydroxyl group

of Tyr408 (Fig. 4A–B). The three BYI09181-bound EcR/USP molecules found in the asymmetric unit of the crystal exhibit a similar interaction pattern with slightly different hydrogen bond lengths.

In the case of the BYI08346-bound EcR, three strong H-bonds are formed between the ligand and the protein, involving residues Thr343, Tyr408 and Asn504. Whereas the ligand nitrogen atom of the imidazole ring at position 3 is H-bonded with Thr343, the carbonyl group close to the B-ring is H-bonded to Tyr408 (Fig. 4C–D). Finally, the amide nitrogen of BYI08346 makes a strong H-bond with the side chain carbonyl group of Asn504. The latter residue is pivotal in the interactions buttressed between the protein and the ligand. Its side chain is in close contact with one side of the isopropyl substitution on

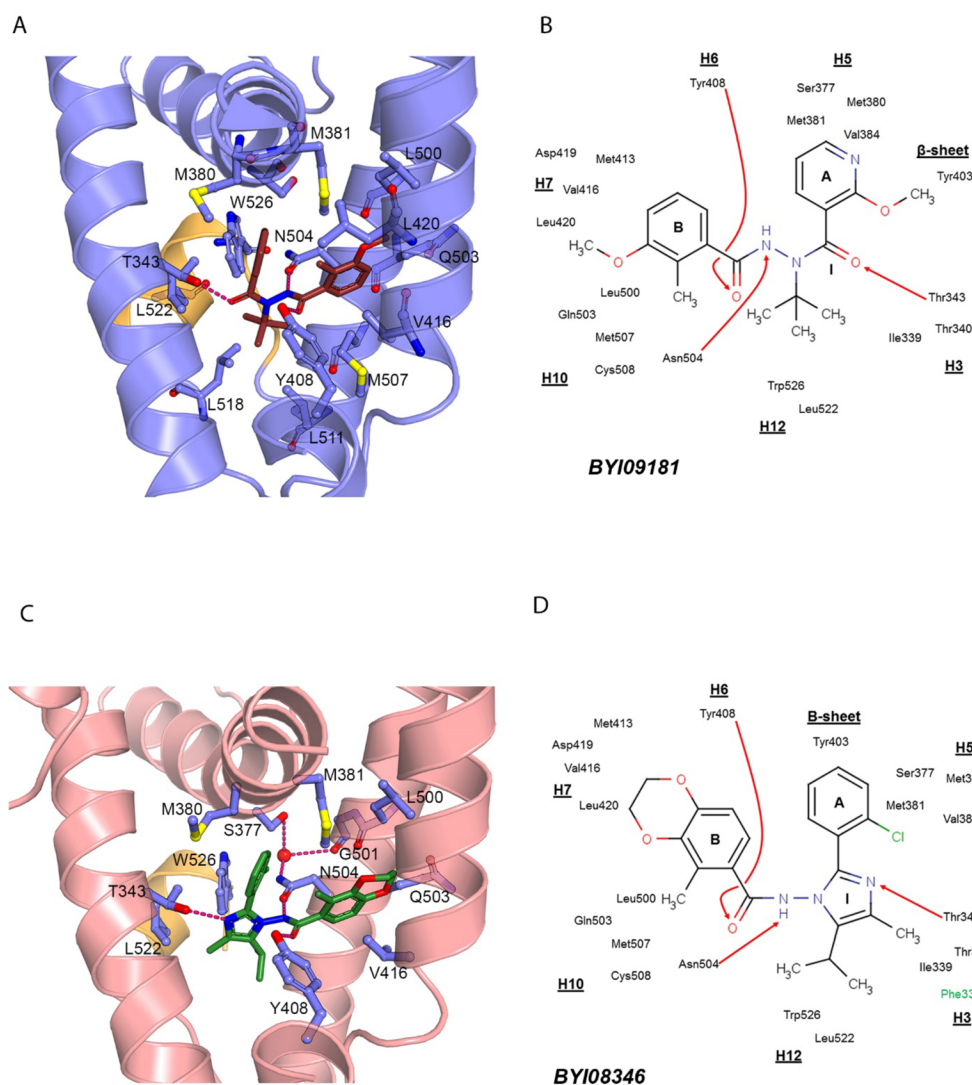


**Fig. 4.** Ligand-binding and interaction networks between the protein and the ligand (A–B) BYI09181 and (C–D) BYI08346. (A–C) Region of the LBP that is in close contacts with (A) BYI09181 and (C) BYI08346. Atom coloring is red for oxygen, blue for nitrogen, yellow for sulfur, pink for carbon in BYI09181, green for carbon in BYI08346. The hydrogen bond interaction network involves residues Thr343, Tyr408 and Asn504. Hydrogen bonds between the ligands BYI09181 and BYI08346 and pocket residues are indicated by red dotted lines. HvEcR-LBP in complex with BYI09181 and BYI08346 is shown with blue and pink ribbons, respectively. (B, D) Schematic representation of the interactions of BYI09181 (B) and BYI08346 (D) with residues of the LBP, where red arrows indicate H-bonds.



the imidazole ring and forms an intricate H-bond interaction network, involving its side chain amide group that is H-bonded to a structural water molecule itself H-bonded to the hydroxyl group of Ser377 and the carbonyl group of Gly501. In addition to the three hydrogen bonds, several key hydrophobic contacts are made between protein residues and BYI08346, as well as  $\pi$ -stacking interactions between the imidazole ring of BYI08346 and the indole ring of Trp526 (Figs. 4C–D). Altogether, a comparison of these two structures with that of BYI06830-bound EcR demonstrates that the hydrogen bond interaction network between each of the synthetic compounds and the residues of the EcR LBP is preserved, even in the case of BYI08346 where an imidazole ring replaces the *tert*-butyl amide moiety of the classical DBH compounds. However, in this case, the hydroxyl group of Thr343 interacts with the nitrogen atom of the imidazole ring of BYI08346 (Figs. 4C–D) and not with the amide carbonyl group as observed in the classical DBH bound EcR structures (Figs. 4A–B).

#### 4. The A- and B-ring positioning of BYI08346 and BYI09181 synthetic compounds

The A-rings of the synthetic compounds BYI08346, BYI09181 and BYI06830 are located in a similar position inside the ligand binding pocket, but show variation in the precise ring orientation and the concomitant location of the ring substituents.

For the classical DBH compound BYI09181, the electron density shows unambiguous positioning of the B-ring substituents, the 3-methoxy substituent oriented towards helix H7 and the 2-methyl group oriented towards the A-ring substituents (Fig. 5A). On the other hand, the experimental data do not allow the unambiguous positioning of the 2-methoxy A-ring substituent which solely from our medium resolution crystallographic data, could adopt two conformations, flipped one with respect to the other, facing either the H12 region (conformer 'h12') or the  $\beta$ -sheet region (conformer 'beta') (Fig. 5A). The conformer 'h12' is characterized by the 2-methoxy A-ring substituent being in close contact to the side chain of Asn504 and the indole ring of Trp526. In contrast, for the conformer 'beta,' the oxygen atom of the 2-methoxy substituent is in close contact to the side chain of Tyr408. Notice that the 3-pyridyl nitrogen of the BYI09181 A-ring substituent is in van der Waals contact to the sulfur atom of Met380 and Met381, these two residues forming a hydrophobic clamp on either side of the A-ring, as seen already for BYI08346.

For the imidazole-type compound BYI08346, the 2-Cl substituent is unambiguously determined from the electron density map (Fig. 5B). It is engaged in a network of H-bond interactions that connect the carbonyl group of the Asn504 side chain with the amide group of the ligand, strongly stabilizing the ligand inside the pocket. Furthermore, this 2-Cl substituent is in close proximity (about 4 Å) of the indole ring of Trp526. The whole A-ring is in van der Waals interactions with two methionine residues in H5 (Met380 and Met381) which are located on either side of the ring and form a clamp (Figs. 4C–D). The B-ring and its 3,4-ethylenedioxy substituent makes hydrophobic interac-

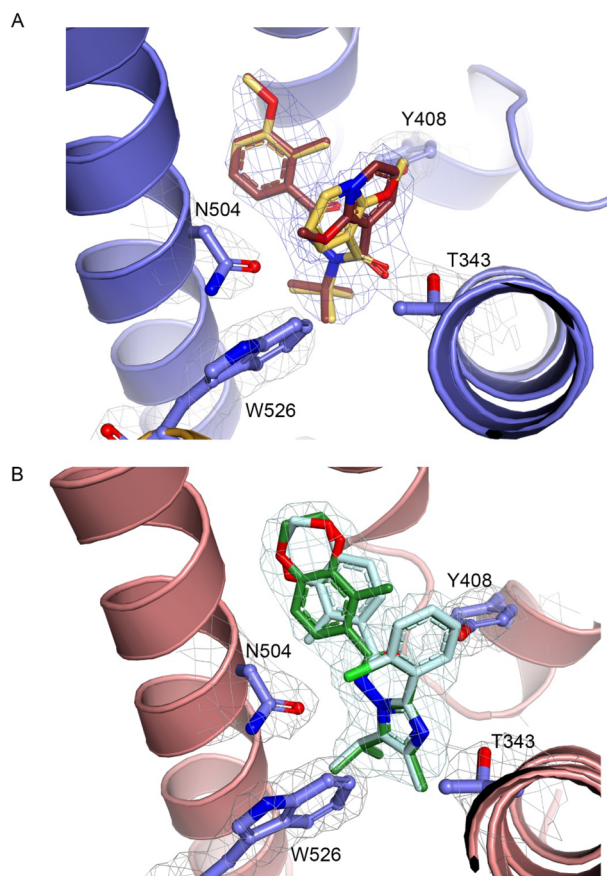


**Fig. 5.** Different conformers of the synthetic agonists BYI09181 or BYI08346 are possible from the electron density map. (A) Electron density map for BYI09181-bound EcR at 2.85 Å resolution for the 'h12' conformer depicted with the pink carbon atoms. The 'beta' conformer of BYI09181 is shown in the map with yellow-orange carbon atoms. (B) Electron density map for BYI08346-bound HvEcR LBD EcR at 3.05 Å resolution for the 'up' conformer depicted with the green carbon atoms. The 'down' conformer of BYI08346 is shown in the map with pale cyan carbon atoms. The three residues forming H-bonds with the ligands, T343, Y408, N504, as well as W526 are shown together with their electron density. The sigmaA weighted  $2F_{\text{obs}} - F_{\text{calc}}$  omit map is shown for the ligand and for the residues, contoured at 1.0  $\sigma$  and overlaid on the final refined models.

tions with residues of the pocket, where the B-ring faces the side chain of Val416 and the ethylenedioxy moiety is in close contact to the side chain of Gln503. However, from the electron density, it is not clear whether the 2-methyl group is oriented up towards Met380/Met381 and the A-ring (conformer 'up') or down towards helix H10 and Gln503 (conformer 'down') (Fig. 5B).

In order to gain insight into the conformational states of either BYI08346 or BYI09181 in the binding site, MD simulations and MM/PBSA calculations were performed. The initial structures for EcR were constructed by complementing the residues and the side chains that were missing in our X-ray crystallographic data (see Materials and Methods). For BYI09181, both conformers 'h12' and 'beta' (Fig. 5A) were considered independently as initial structures. For BYI08346, both conformers 'up'



**Table 2.** Binding free energy of BYI08346 and BYI09181 conformers calculated by MM/PBSA

Conformer	Calculated $\Delta G_{\text{bind}}$ (kcal/mol)			
	1st	2nd	3rd	Mean $\pm$ S.D.
BYI09181 'h12'	−4.23	−5.27	−8.09	−5.86 $\pm$ 2.00
BYI09181 'beta'	−6.42	−7.45	−0.64	−4.84 $\pm$ 3.67
BYI08346 'down'	−5.46	1.38	−5.92	−3.34 $\pm$ 4.09
BYI08346 'up'	−4.91	−6.39	−3.61	−4.97 $\pm$ 1.39

and 'down' were used as initial structures (Fig. 5B). For each of four ligand–receptor complexes, we executed three independent 1.5-ns MD simulations. The resulting MD trajectories were subjected to MM/PBSA calculations to estimate the free energy of ligand–receptor binding ( $\Delta G_{\text{bind}}$ ). As shown in Table 2, for BYI09181, conformer 'h12' is more stable than conformer 'beta.' For BYI08346, conformer 'up' is more stable than conformer 'down.'

## Discussion

The published structures of EcR bound to BYI06830 and PonA<sup>19)</sup> set the mark for a novel concept in the field of nuclear receptors, namely that of receptor adaptability and plasticity towards its bound ligand. These structural observations helped rationalizing the remarkable capacity of EcR to bind to and be activated by ligands of completely different chemical and structural types. Since these first observations, a few other crystal structures of different nuclear receptors (LXR, VDR, ER, GR) have been published that emphasize the adaptability of nuclear receptors to their ligand.<sup>40–46)</sup> One of the most striking examples is GR that opens up a new pocket upon binding of deacylcortivazol in the upper part of the receptor close to helix H1.<sup>45)</sup> In this work, we report on the adaptability of EcR when bound to two different synthetic agonists, a classical DBH compound (BYI09181) and an imidazole-type derivative (BYI08346) which is structurally related to OXA compounds. These two structures demonstrate that drastic structural adaptations occur in order to bind these synthetic agonists. Upon binding of the DBH ligand BYI09181 and the imidazole-type compound BYI08346, HvEcR adapts by rearranging the three-stranded  $\beta$ -sheet and the helix H2 in a way similar to what was observed for the BYI06830-bound EcR structure.<sup>19)</sup>

The binding mode of these two synthetic agonists is conserved compared to that of the DBH compound BYI06830 and encompasses three hydrogen bonds formed between the ligand and residues Thr343, Tyr408 and Asn504. Furthermore, the synthetic ligands occupy a similarly shaped binding pocket, despite modifications on the A- and B-rings and the more drastic architectural change of BYI08346 which contains an imidazole ring compared to the classical hydrazide centre. In each of the three crystal structures, the synthetic ligand does not make close contact with residues belonging to the region encompassing helices H1 and H6 and the  $\beta$ -sheet, a part of the LBD occupied by the

steroid core of the ecdysteroids when they are bound to EcR. In addition, although certain regions of the receptor (such as H5 and H10) are common among the two types of LBPs observed for ecdysteroids and for DBH compounds, a few residues interact specifically with the synthetic compounds. In particular, Ser377 in H5 makes hydrophobic contacts with synthetic agonists through their A-ring and not with ecdysteroids, and the residues Leu500 and Gln503 at the carboxy-terminus of H10 exclusively interact with synthetic compounds through their B-ring.

Despite the similarity in the mechanisms of structural adaptation already observed for the BYI06830-bound EcR structure, the two additional structures described in this paper give more accurate details on the interaction between synthetic compounds and their cognate receptor. For example, we can unambiguously answer the issue of which DBH conformational isomer is selected inside the EcR ligand binding pocket. Computational studies of free DBH compounds identified four conformational clusters: *i.e.*, extended *Z,Z*-, hooked *E,Z*-, folded *Z,E*-, and stacked *E,E*-conformers (Suppl. Figure 1A).<sup>17,47,48)</sup> Among these, the stacked *E,E*- and the folded *Z,E*-conformers were identified as two low-energy clusters, although the precise energetic rankings depend to a large degree upon substituent patterns of the aromatic rings, in particular *ortho*-substitution. Furthermore, each cluster may occur in enantiomeric forms (*M*- and *P*-helicity), due to the substantial barrier to the N–N bond rotation on the time scale of the receptor binding event (Suppl. Figure 1B). Thus, DBH molecules adopt a maximum of eight conformational clusters. In the BYI06830-bound structure (PDB: 1R20), both of folded *Z,E*-conformations with *M*- and *P*-helicity could equally be accommodated inside the pocket; therefore, we provisionally assigned the folded *Z,E*-conformer with *P*-helicity to the ligand geometry.<sup>19)</sup> The structure of BYI08346-bound EcR reported here, however, allows the unambiguous identification of the stereochemical configuration of this compound inside the LBP. In fact, the planar rigidity of the imidazole ring of BYI08346 defines the ligand topology and the pattern of interaction with the protein. In this case, the carbonyl moiety of the B-ring is H-bonded to Tyr408 and the B-ring amide moiety makes a hydrogen bond with the carbonyl group of the side chain of Asn504. In this configuration, the side chain amide group of Asn504 in H11 makes an electrostatic interaction of NH- $\pi$  type with the aromatic ring of the strictly conserved tryptophan residue Trp526 inside H12. In addition, the electron density at the level of the BYI09181 ligand indicates that the folded conformer with *M*-helicity fits better inside the cavity than that with *P*-helicity, which results in an identical H-bond interaction pattern as observed for BYI08346. The folded *Z,E*-conformer with *M*-helicity is reasonable because this conformation allows the hydrogen bond between the carbonyl group close to the B-ring (H-bond acceptor) and the hydroxy group of Y408 (H-bond donor), which is energetically more favorable than that observed for the folded conformation with *P*-helicity. Thus, the detailed observation of the binding patterns of BYI08346 and BYI09181 strongly

suggests that the binding mode of DBH compounds in EcR is a folded *Z,E*-conformation with *M*-helicity.

Most importantly, the structures of BYI-bound EcR described here allow deeper insight into the molecular springs that EcR uses to adapt and bind to various synthetic compounds with high affinity. The most significant one is the spreading of a gap between helices H7 and H10. Interestingly, in order for the LBD to accommodate the synthetic agonists, a cleft opens up between helices H7 and H10 and allows the insertion of the B-ring of the synthetic compounds. A wide cleft is observed for BYI06830 and BYI08346, both bearing the same 3,4-ethylenedioxy substitution on the B-ring. In contrast, BYI09181 possesses 2-methyl and 3-methoxy substituents on the B-ring, which are smaller than those on the B-ring of BYI06830 and BYI08346. Consequently, the cleft between helices H7 and H10 is narrower than those observed in the BYI06830- and BYI08346-bound EcR structures. This observation answers the question of whether the binding mode of the bulky B-ring substitutions of BYI06830 is representative of other members of the synthetic agonists, some of which have smaller B-ring substitutions.<sup>22)</sup> The degree of adaptability provided by this mechanism has limitations though, as suggested by activity data of compounds with variously sized B-ring substitutions that show a decrease and even a lack of activity for compounds bearing very bulky substitutions on the B-ring.<sup>14)</sup> Importantly, this region of the LBP is filled with structural water molecules in the structures of *Heliothis virescens* EcR bound to 20E<sup>20)</sup> and *Tribolium castaneum* EcR bound to PonA,<sup>21)</sup> emphasizing the alternative structural role of this region when bound to synthetic compounds. The use of the water channel molecules in the design of selected NR ligands has been demonstrated in other nuclear receptors (VDR and LRH-1 among others). In the case of 1 $\alpha$ ,25-dihydroxyvitamin D3 (1 $\alpha$ ,25(OH)<sub>2</sub>D<sub>3</sub>)-bound VDR, three water molecules are observed at the level of the A-ring. On the other hand, 2 $\alpha$ -substituted 1 $\alpha$ ,25(OH)<sub>2</sub>D<sub>3</sub> analogues do or do not exhibit these structural water molecules depending on the nature of the 2 $\alpha$ -substitution, with ligand affinities reflecting the balance between the loss of water-mediated H-bonds, additional van der Waals contacts and entropic effects.<sup>49)</sup> In the case of LRH-1, a network of conserved water molecules near the LBP was proven to be important for activation by the agonist ligand.<sup>40)</sup> Networks of conserved water molecules which play important functional and structural roles have been identified in several other protein complexes, such as MHC class-I molecules.<sup>50)</sup> Considering explicitly relevant water molecules in protein binding sites has been considered as a promising approach for increasing the efficiency of rational drug design strategies.<sup>51–53)</sup> Our data provide a nice example of how the relevant structural water molecules of ecdysteroid-bound EcR have been displaced by the synthetic insecticide compounds, reproducing the feature of structural stabilization brought by the water network by the specific functional group of the synthetic DBH insecticides and the OXA-type of compounds.

The molecular spring function of helices H7 and H10 also deepens our interpretation of the previous QSAR results. For ex-

ample, we formulated the following QSAR equation for DBH ligands with varied substituents at the 4-position on the B-ring<sup>54)</sup>

$$\text{pIC}_{50} = 0.607 \log P - 0.822\sigma - 0.367 \Delta B_1 + 5.502 \quad (1)$$

$$n = 17, \quad r^2 = 0.914, \quad s = 0.243$$

where  $\text{pIC}_{50}$  is the ligand–receptor binding affinity evaluated in lepidopteran Sf-9 cells,  $\log P$  is the hydrophobicity, being equivalent to the hydrophobicity parameter ( $\pi$ ) of substituents in this compound set,  $\sigma$  is the Hammett substituent constant, and  $\Delta B_1$  is the STERIMOL minimal width parameter of substituents relative to hydrogen. Equation (1) indicates that hydrophobic and electron-donating substituents at position 4 of the B-ring enhance the binding affinity, while bulky substituents at this position are sterically unfavorable. It is generally accepted that the  $\log P$  term in QSAR equations correspond to the ligand desolvation process, which must occur prior to the ligand–receptor association. Taken together with the detailed structural observations made in this study, the positive coefficient of the  $\log P$  term in Eq. (1) is likely to have three implications: (i) the reduced desolvation cost for hydrophobic substituents, (ii) the entropic gain upon displacing the structural water molecules, and (iii) the van der Waals contacts of 4-substituents with the cleft-forming amino acids, which partly compensate for the enthalpic loss resulting from the disruption of the water-mediated H-bonding network. This three-faced nature is likely the reason why the  $\log P$  term is the most significant parameter in Eq. (1), accounting for approximately 73% of the total activity deviation.

In addition to this molecular spring of adaptability, a second mechanism, although less significant, is used by EcR to accommodate the synthetic ligands. This is shown by comparing the LBP of BYI08346 with those of BYI09181 and BYI06830 at the level of the hydrazide center. The *tert*-butyl group of BYI09181 and BYI06830 and the isopropyl group of BYI08346 fit well inside the hydrophobic part of LBP constituted by helices H3, H11 and H12 and the loops L6–7 and L11–12 and make extensive hydrophobic contacts with residues of this region. However, in the case of BYI08346, the imidazole ring and its methyl substitution at position 4 extends into a part of the LBP that is not interacting with DBH compounds. These moieties are then accommodated inside the LBP by a concomitant outward movement of the helices H3 and H6 and the loop connecting H6 to H7. Thus, EcR demonstrates an additional level of plasticity that might be used by the receptor to bind ligands with large central modules found for example in amidoketones<sup>17,18,55,56)</sup> and in some DBH analogs with bulky *N*-substituents.<sup>57)</sup>

## Conclusions

The binding of DBH- and imidazole-type compounds to EcR involves a remarkable remodeling of the protein. In addition to the major remodeling features, such as the  $\beta$ -sheet remodeling and the loss of helix H2, the crystal structures of EcR in complex with BYI09181 and BYI08346 pinpoint a critical region for adaptation, namely the region delineated by helices H7 and

H10 that opens up in order to tightly fit the B-ring to an extent that depends on the bulkiness of the B-ring substituent. The potentiality of this region to act as a critical molecular adaptation spring is in fact imprinted in the structure of *Heliothis* and *Tribolium* EcR bound to ecdysteroids, where this part of the LBP exhibits a channel filled by relevant structural water molecules.

The B-ring and its substituents make extensive van der Waals contacts with LBP residues, compensating to some extent for the enthalpic penalty arising from the lack of the water-mediated H-bond interaction network observed for ecdysteroid-bound EcR. It is likely that the binding of DBH and imidazole-like compounds is then further promoted by the hydrophobic B-ring substituents, which benefit from the reduced desolvation cost and the entropic gain as compared to ecdysteroids. In conclusion, this work illustrates how a structurally important water channel present in the structure of EcR bound to its endogenous hormone can be used for the binding of synthetic agonists, exemplifying a concept that may be essential in the *de novo* ligand design.

### Acknowledgements

We thank the Structural Biology and Genomics Platform at IGBMC and G. Holmwood and M. Schindler (Bayer CropScience, Monheim, Germany) for discussion and André Mitschler for help in data collection. The authors acknowledge the support and the use of the French Infrastructure for Integrated Structural Biology FRISBI ANR-10-INSB-05-01 and Instruct-ERIC, a Landmark ESFRI project. The work was supported in part by Bayer CropScience (Monheim, Germany) and by the grant ANR-10-LABX-0030-INRT, a French State fund managed by the Agence Nationale de la Recherche under the frame program Investissements d'Avenir ANR-10-IDEX-0002-02. This work was also supported in part by JSPS KAKENHI Grant Numbers JP16K07625, JP17J01486, and JP19K06051.

### Conflict of Interest

The authors declare that they have no conflict of interest.

### Author Contributions

IMLB, DM and YN designed the study and supervised research; IMLB, CB, YN, TY and KM wrote the manuscript; CB, AGM, KM, TY, YN and IMLB performed the experiments and analysed the data.

### Database

The coordinates and structure factors have been deposited in the Protein Data Bank under the accession codes 7BJU for BYI08346 and 7BJV for BYI09181.

### Electronic supplementary materials

The online version of this article contains supplementary materials (Supplemental Table 1 and Fig. 1), which are available at <http://www.jstage.jst.go.jp/browse/jpestics/>.

### References

- 1) M. Miyashita, K. Matsushita, S. Nakamura, S. Akahane, Y. Nakagawa and H. Miyagawa: LC/MS/MS identification of 20-hydroxyecdysone in a scorpion (*Liocheles australasiae*) and its binding affinity to *in vitro*-translated molting hormone receptors. *Insect Biochem. Mol. Biol.* **41**, 932–937 (2011).
- 2) F. Lachaise and R. Lafont: Ecdysteroid metabolism in a crab: *Carcinus maenas* L. *Steroids* **43**, 243–259 (1984).
- 3) R. J. Hill, I. M. L. Billas, F. Bonneton, L. D. Graham and M. C. Lawrence: Ecdysone receptors: From the Ashburner model to structural biology. *Annu. Rev. Entomol.* **58**, 251–271 (2013).
- 4) M. R. Koelle, W. S. Talbot, W. A. Segraves, M. Bender, P. Cherbas and D. S. Hogness: The drosophila EcR gene encodes an ecdysone receptor, a new member of the steroid receptor superfamily. *Cell* **67**, 59–77 (1991).
- 5) H. E. Thomas, H. G. Stunnenberg and A. F. Stewart: Heterodimerization of the Drosophila ecdysone receptor with retinoid X receptor and ultraspiracle. *Nature* **362**, 471–475 (1993).
- 6) T.-P. Yao, B. M. Forman, Z. Jiang, L. Cherbas, J.-D. Chen, M. McKeown, P. Cherbas and R. M. Evans: Functional ecdysone receptor is the product of EcR and ultraspiracle genes. *Nature* **366**, 476–479 (1993).
- 7) T.-P. Yao, W. A. Segraves, A. E. Oro, M. McKeown and R. M. Evans: Drosophila ultraspiracle modulates ecdysone receptor function via heterodimer formation. *Cell* **71**, 63–72 (1992).
- 8) Y. Nakagawa and V. C. Henrich: Arthropod nuclear receptors and their role in molting. *FEBS J.* **276**, 6128–6157 (2009).
- 9) S. E. Fahrbach, G. Smagghe and R. A. Velarde: Insect nuclear receptors. *Annu. Rev. Entomol.* **57**, 83–106 (2012).
- 10) T. S. Dhadialla, G. R. Carlson and D. P. Le: New insecticides with ecdysteroidal and juvenile hormone activity. *Annu. Rev. Entomol.* **43**, 545–569 (1998).
- 11) Y. Nakagawa: Nonsteroidal ecdysone agonists. *Vitam. Horm.* **73**, 131–173 (2005).
- 12) G. R. Carlson, T. S. Dhadialla, R. Hunter, R. K. Jansson, C. S. Jany, Z. Lidert and R. A. Slawski: The chemical and biological properties of methoxyfenozide, a new insecticidal ecdysteroid agonist. *Pest Manag. Sci.* **57**, 115–119 (2001).
- 13) Y. Sawada, T. Yanai, H. Nakagawa, Y. Tsukamoto, Y. Tamagawa, S. Yokoi, M. Yanagi, T. Toya, H. Sugizaki, Y. Kato, H. Shirakura, T. Watanabe, Y. Yajima, S. Kodama and A. Masui: Synthesis and insecticidal activity of benzoheterocyclic analogues of *N'*-benzoyl-*N*-(*tert*-butyl)benzohydrazide: Part 3. Modification of *N*-*tert*-butylhydrazine moiety. *Pest Manag. Sci.* **59**, 49–57 (2003).
- 14) Y. Sawada, T. Yanai, H. Nakagawa, Y. Tsukamoto, S. Yokoi, M. Yanagi, T. Toya, H. Sugizaki, Y. Kato, H. Shirakura, T. Watanabe, Y. Yajima, S. Kodama and A. Masui: Synthesis and insecticidal activity of benzoheterocyclic analogues of *N'*-benzoyl-*N*-(*tert*-butyl)benzohydrazide: Part 2. Introduction of substituents on the benzene rings of the benzoheterocycle moiety. *Pest Manag. Sci.* **59**, 36–48 (2003).
- 15) Y. Nakagawa, R. E. Hormann and G. Smagghe: "SAR and QSAR studies for *in vivo* and *in vitro* activities of ecdysone agonists." In *Ecdysone: Structures and Functions*, ed. by G. Smagghe, Springer, pp. 475–509, 2009.
- 16) Y. Nakagawa and T. Harada: "Advanced Screening to Identify Novel Pesticides." In *Advanced Technologies for Managing Insect Pests*, eds. by I. Ishaaya, R. Palli, A. R. Horowitz, Springer, Dordrecht, The Netherlands, pp. 135–163, 2013.
- 17) L. Dinan and R. E. Hormann: "Ecdysteroid Agonists and Antagonists." In *Comprehensive Molecular Insect Science*, eds. by L. I. Gilbert, K. Iatrou, and S. S. Gill, Elsevier, Amsterdam, pp. 198–242, 2004.
- 18) L. Dinan, Y. Nakagawa and R. E. Hormann: Structure–activity relationships of ecdysteroids and non-steroidal ecdysone agonists. *Adv. Insect Physiol.* **43**, 251–298 (2012).
- 19) I. M. L. Billas, T. Iwema, J. M. Garnier, A. Mitschler, N. Rochel and

- D. Moras: Structural adaptability in the ligand-binding pocket of the ecdysone hormone receptor. *Nature* **426**, 91–96 (2003).
- 20) C. Browning, E. Martin, C. Loch, J. M. Wurtz, D. Moras, R. H. Stote, A. P. Dejaegere and I. M. L. Billas: Critical role of desolvation in the binding of 20-hydroxyecdysone to the ecdysone receptor. *J. Biol. Chem.* **282**, 32924–32934 (2007).
  - 21) T. Iwema, I. M. L. Billas, Y. Beck, F. Bonneton, H. Nierengarten, A. Chaumot, G. Richards, V. Laudet and D. Moras: Structural and functional characterization of a novel type of ligand-independent RXR-USP receptor. *EMBO J.* **26**, 3770–3782 (2007).
  - 22) J. A. Carmichael, M. C. Lawrence, L. D. Graham, P. A. Pilling, V. C. Epa, L. Noyce, G. Lovrecz, D. A. Winkler, A. Pawlak-Skrzecz, R. E. Eaton, et al.: The X-ray structure of a hemipteran ecdysone receptor ligand-binding domain: comparison with a lepidopteran ecdysone receptor ligand-binding domain and implications for insecticide design. *J. Biol. Chem.* **280**, 22258–22269 (2005).
  - 23) B. Ren, T. S. Peat, V. A. Streltsov, M. Pollard, R. Fernley, J. Grusovin, S. Seabrook, P. Pilling, T. Phan, L. Lu, G. O. Lovrecz, L. D. Graham and R. J. Hill: Unprecedented conformational flexibility revealed in the ligand-binding domains of the *Bovicola ovis* ecdysone receptor (EcR) and ultraspiracle (USP) subunits. *Acta Crystallogr. D Biol. Crystallogr.* **70**, 1954–1964 (2014).
  - 24) M. Maletta, I. Orlov, P. Roblin, Y. Beck, D. Moras, I. M. L. Billas and B. P. Klaholz: The palindromic DNA-bound USP/EcR nuclear receptor adopts an asymmetric organization with allosteric domain positioning. *Nat. Commun.* **5**, 4139 (2014).
  - 25) I. M. L. Billas and D. Moras: Allosteric Controls of Nuclear receptor function in the regulation of transcription. *J. Mol. Biol.* **425**, 2317–2329 (2013).
  - 26) Z. Otwinowski and W. Minor: Processing of X-ray diffraction data collected in oscillation mode. *Methods Enzymol.* **276**, 307–326 (1997).
  - 27) A. Vagin and A. Teplyakov: MOLREP: An automated program for molecular replacement. *J. Appl. Cryst.* **30**, 1022–1035 (1997).
  - 28) J. Navaza: Amore: An automated package for molecular replacement. *Acta Crystallogr. A* **50**, 157–163 (1994).
  - 29) A. T. Brünger, P. D. Adams, G. M. Clore, W. L. DeLano, P. Gros, R. W. Grosse-Kunstleve, J. S. Jiang, J. Kuszewski, M. Nilges, N. S. Pannu, et al.: Crystallography & NMR System: A new software suite for macromolecular structure determination. *Acta Cryst. D* **54**, 905–. *Methods Enzymol.* **276**, 307–326 (1998).
  - 30) T. A. Jones, J. Y. Zou, S. W. Cowan and M. Kjeldgaard: Improved methods for building protein models in electron density maps and the location of errors in these models. *Acta Crystallogr. A* **47**, 110–119 (1991).
  - 31) P. D. Adams, P. V. Afonine, G. Bunkoczi, V. B. Chen, I. W. Davis, N. Echols, J. J. Headd, L.-W. Hung, G. J. Kapral, R. W. Grosse-Kunstleve, A. J. McCoy, N. W. Moriarty, R. Oeffner, R. J. Read, D. C. Richardson, J. S. Richardson, T. C. Terwilliger and P. H. Zwart: PHENIX: A comprehensive Python-based system for macromolecular structure solution. *Acta Crystallogr. D Biol. Crystallogr.* **66**, 213–221 (2010).
  - 32) P. Emsley, B. Lohkamp, W. G. Scott and K. Cowtan: Features and development of Coot. *Acta Crystallogr. D Biol. Crystallogr.* **66**, 486–501 (2010).
  - 33) V. B. Chen, W. B. Arendall III, J. J. Headd, D. A. Keedy, R. M. Immormino, G. J. Kapral, L. W. Murray, J. S. Richardson and D. C. Richardson: MolProbity: All-atom structure validation for macromolecular crystallography. *Acta Crystallogr. D Biol. Crystallogr.* **66**, 12–21 (2010).
  - 34) G. J. Kleywegt and T. A. Jones: Detection, delineation, measurement and display of cavities in macromolecular structures. *Acta Crystallogr. D Biol. Crystallogr.* **50**, 178–185 (1994).
  - 35) S. Horoiwa, T. Yokoi, S. Masumoto, S. Minami, C. Ishizuka, H. Kishikawa, S. Ozaki, S. Kitsuda, Y. Nakagawa and H. Miyagawa: Structure-based virtual screening for insect ecdysone receptor ligands using MM/PBSA. *Bioorg. Med. Chem.* **27**, 1065–1075 (2019).
  - 36) G. Holmwood and M. Schindler: Protein structure based rational design of ecdysone agonists. *Bioorg. Med. Chem.* **17**, 4064–4070 (2009).
  - 37) R. E. Hormann and O. Chortyk: Oxadiazoline ligands for modulating the expression of exogenous genes via an ecdysone receptor. (US, 2004), 10/783,810.
  - 38) I. M. L. Billas, L. Moulinier, N. Rochel and D. Moras: Crystal structure of the ligand binding domain of the ultraspiracle protein USP, the ortholog of RXRs in insects. *J. Biol. Chem.* **276**, 7465–7474 (2001).
  - 39) I. M. L. Billas, C. Browning, M. C. Lawrence, L. D. Graham, D. Moras and R. J. Hill: “The Structure and Function of Ecdysone Receptors.” In *Ecdysone: Structures and Functions*, ed. by G. Smagghe, Springer Science+Business Media B.V., chap. 13, pp. 335–360, 2009.
  - 40) S. G. Mays, C. D. Okafor, R. J. Whitby, D. Goswami, J. Stec, A. R. Flynn, M. C. Dugan, N. T. Jui, P. R. Griffin and E. A. Ortlund: Crystal structures of the nuclear receptor, liver receptor homolog 1, bound to synthetic agonists. *J. Biol. Chem.* **291**, 25281–25291 (2016).
  - 41) J. C. Nwachukwu, S. Srinivasan, Y. Zheng, S. Wang, J. Min, C. Dong, Z. Liao, J. Nowak, N. J. Wright, R. Houtman, K. E. Carlson, J. S. Josan, O. Elemento, J. A. Katzenellenbogen, H. B. Zhou and K. W. Nettles: Predictive features of ligand-specific signaling through the estrogen receptor. *Mol. Syst. Biol.* **12**, 864 (2016).
  - 42) K. W. Nettles, J. B. Bruning, G. Gil, E. E. O’Neill, J. Nowak, Y. Guo, Y. Kim, E. R. DeSombre, R. Dillis, R. N. Hanson, et al.: Structural plasticity in the oestrogen receptor ligand-binding domain. *EMBO Rep.* **8**, 563–568 (2007).
  - 43) F. Ciesielski, N. Rochel, A. Mitschler, A. Kouzmenko and D. Moras: Structural investigation of the ligand binding domain of the zebrafish VDR in complexes with  $1\alpha,25(\text{OH})_2\text{D}_3$  and Gemini: purification, crystallization and preliminary X-ray diffraction analysis. *J. Steroid Biochem. Mol. Biol.* **89–90**, 55–59 (2004).
  - 44) M. Farnegardh, T. Bonn, S. Sun, J. Ljunggren, H. Ahola, A. Wilhelmsson, J. A. Gustafsson and M. Carlquist: The three dimensional structure of the liver X receptor beta reveals a flexible ligand binding pocket that can accommodate fundamentally different ligands. *J. Biol. Chem.* **278**, 38821–38828 (2003).
  - 45) K. Suino-Powell, Y. Xu, C. Zhang, Y. G. Tao, W. D. Tolbert, S. S. Simons Jr. and H. E. Xu: Doubling the size of the glucocorticoid receptor ligand binding pocket by deacylcortivazol. *Mol. Cell. Biol.* **28**, 1915–1923 (2008).
  - 46) M. Togashi, S. Borngraeber, B. Sandler, R. J. Fletterick, P. Webb and J. D. Baxter: Conformational adaptation of nuclear receptor ligand binding domains to agonists: Potential for novel approaches to ligand design. *J. Steroid Biochem. Mol. Biol.* **93**, 127–137 (2005).
  - 47) R. E. Hormann, L. Dinan and P. Whiting: Superimposition evaluation of ecdysteroid agonist chemotypes through multidimensional QSAR. *J. Comput. Aided Mol. Des.* **17**, 135–153 (2003).
  - 48) J.-M. Wurtz, B. Guillot, J. Fagart, D. Moras, K. Tietjen and M. Schindler: A new model for 20-hydroxyecdysone and dibenzoylhydrazine binding: A homology modeling and docking approach. *Protein Sci.* **9**, 1073–1084 (2000).
  - 49) S. Hourai, T. Fujishima, A. Kittaka, Y. Suhara, H. Takayama, N. Rochel and D. Moras: Probing a water channel near the A-ring of receptor-bound  $1\alpha,25$ -dihydroxyvitamin D<sub>3</sub> with selected  $2\alpha$ -substituted



- analogues. *J. Med. Chem.* **49**, 5199–5205 (2006).
- 50) K. Ogata and S. J. Wodak: Conserved water molecules in MHC class-I molecules and their putative structural and functional roles. *Protein Eng.* **15**, 697–705 (2002).
- 51) C. Barillari, J. Taylor, R. Viner and J. W. Essex: Classification of water molecules in protein binding sites. *J. Am. Chem. Soc.* **129**, 2577–2587 (2007).
- 52) A. Amadasi, J. A. Surface, F. Spyraakis, P. Cozzini, A. Mozzarelli and G. E. Kellogg: Robust classification of “Relevant” water molecules in putative protein binding sites. *J. Med. Chem.* **51**, 1063–1067 (2008).
- 53) G. Klebe: Applying thermodynamic profiling in lead finding and optimization. *Nat. Rev. Drug Discov.* **14**, 95–110 (2015).
- 54) T. Ogura, Y. Nakagawa, C. Minakuchi and H. Miyagawa: QSAR for binding affinity of substituted dibenzoylhydrazines to intact Sf-9 Cells. *J. Pestic. Sci.* **30**, 1–6 (2005).
- 55) C. M. Tice, R. E. Hormann, C. S. Thompson, J. L. Friz, C. K. Cavanaugh, E. L. Michelotti, J. Garcia, E. Nicolas and F. Albericio: Synthesis and SAR of  $\alpha$ -acylaminoketone ligands for control of gene expression. *Bioorg. Med. Chem. Lett.* **13**, 475–478 (2003).
- 56) C. M. Tice, R. E. Hormann, C. S. Thompson, J. L. Friz, C. K. Cavanaugh and J. A. Saggars: Optimization of  $\alpha$ -acylaminoketone ecdysone agonists for control of gene expression. *Bioorg. Med. Chem. Lett.* **13**, 1883–1886 (2003).
- 57) R. E. Hormann, B. Li: Chiral Diacylhydrazine Ligands for Modulating the Expression of Exogenous Genes via an Ecdysone Receptor Complex, US8,076,517, 2011.
- 58) C. Browning: Structural Studies of Insect Nuclear Receptors. PhD thesis. Aspects Moléculaires et Cellulaires de la Biologie, Université de Strasbourg, 2007.